Subshell-selective x-ray studies of radiative recombination of U^{92+} ions with electrons for very low relative energies

D. Banaś,[1] M. Pajek,[1] A. Surzhykov,[2] Th. Stöhlker,[2,3,4] C. Brandau,[3,5] A. Gumberidze,[6] C. Kozhuharov,[3] H. F. Beyer,[3] S. Böhm,[5] F. Bosch,[3] M. Czarnota,[1] S. Chatterjee,[3,*] J.-Cl. Dousse,[7] S. Fritzsche,[2,8] S. Hagmann,[3] D. Liesen,[3] P. H. Mokler,[3] A. Müller,[5] A. Kumar,[3] R. Reuschl,[3] D. Sierpowski,[9] U. Spillmann,[3] J. Szlachetko,[1,7] S. Tashenov,[2,10] S. Trotsenko,[2,3] P. Verma,[3] and A. Warczak[9]

[1]*Institute of Physics, Jan Kochanowski University, PL-25-406 Kielce, Poland*
[2]*Helmholtz-Institut Jena, D-07743 Jena, Germany*
[3]*GSI Helmholtzzentrum für Schwerionenforschung, D-64291 Darmstadt, Germany*
[4]*Institut für Optik und Quantenelektronik, Friedrich-Schiller-Universität Jena, D-07743 Jena, Germany*
[5]*Institut für Atom und Molekülphysik, Justus-Liebig-Universität, D-35392 Giessen, Germany*
[6]*ExtreMe Matter Institute EMMI and Research Division, GSI Helmholtzzentrum für Schwerionenforschung, D-64291 Darmstadt, Germany*
[7]*Department of Physics, University of Fribourg, CH-1700 Fribourg, Switzerland*
[8]*Theoretisch-Physikalisches Institut, Friedrich-Schiller-Universität Jena, D-07743 Jena, Germany*
[9]*Institute of Physics, Jagiellonian University, PL-30-059 Cracow, Poland*
[10]*Physikalisches Institut der Universität Heidelberg, D-69120 Heidelberg, Germany*

(Received 13 July 2015; published 21 September 2015)

Radiative recombination (RR) into the K shell and L subshells of U^{92+} ions interacting with cooling electrons has been studied in an x-ray RR experiment at the electron cooler of the Experimental Storage Ring at GSI. The measured radiative recombination rate coefficients for electron-ion relative energies in the range 0–1000 meV demonstrate the importance of relativistic effects. The observed asymmetry of the measured K-RR x-ray emission with respect to the cooling energy, i.e., zero average relative velocity ($\langle v_{\rm rel}\rangle = 0$), are explained by fully relativistic RR calculations. With our new approach, we show that the study of the angular distribution of RR photons for different relative energies opens new perspectives for detailed understanding of the RR of ions with cooling electrons in cold magnetized plasma.

DOI: 10.1103/PhysRevA.92.032710 PACS number(s): 34.80.Lx, 31.30.jc, 32.30.Rj, 29.20.db

I. INTRODUCTION

Radiative recombination (RR) is one of the most fundamental processes occurring in collisions of highly charged ions with electrons. In this process a free electron is captured into a bound state of an ion with simultaneous photon emission, which can be written as follows:

$$A^{q+} + e(E) \rightarrow A^{(q-1)+}(n) + \hbar\omega. \quad (1)$$

The emitted photon carries off the energy difference $\hbar\omega = E - E_n$ between the continuum state with the energy E and the bound electron state E_n with principal quantum number n. Detailed nonrelativistic quantum mechanical descriptions of RR were developed by Stobbe [1] and Bethe and Salpeter [2].

During the last decades the RR was actively studied in various aspects related to atomic and plasma physics, astrophysics, and accelerator physics (see, for example, Refs. [3–14]). In the 1990s, with the introduction of high quality cold electron targets for merged-beam experiments detailed experimental studies of RR became possible. Significant progress could be achieved only when the electron cooling technique was introduced to ion storage rings. An electron cooler provides an intense cold electron beam which is merged with the ion beam circulating in the ring. It is used to cool the stored ion beam by elastic electron-ion collisions but can also be employed as an electron target to study both RR and dielectronic electron-ion recombination (DR) at relative energies reaching down to the μeV range.

The first RR experiment was performed with merged electron and ion beams in a single-pass arrangement [15]. In later RR experiments performed at different heavy ion storage rings (TSR, CRYRING, ESR) for a broad range of bare ions, ranging from He^{2+} to U^{92+} [16–22], total recombination rate coefficients were measured by detecting the recombined down-charged ions. In these experiments total rate coefficients versus the relative electron energy were determined integral over all empty shells up to the field ionization limit $n_f \gg 1$ appearing due to the motional electric fields present in the bending magnets of the ring. These experiments revealed that the measured recombination rate coefficients substantially exceed the theoretical predictions for RR at relative electron energies below the transverse electron beam temperature $kT_\perp$. This, so-called, "enhancement" effect is well evidenced experimentally for bare ions, up to U^{92+} [22] and also for many-electron ions. Yet, in the latter case, resonances from dielectronic recombination may additionally contribute to the rate coefficient [23]. Additionally, a decisive influence of the magnetic electron-guiding field as well as the longitudinal and transversal electron beam temperatures $kT_\parallel \ll kT_\perp$ on the measured RR rates was observed [21,22], which is also not expected from RR theory. Despite many attempts [3,4,21,24] to explain the above mentioned effects they are still not fully understood. However, it was pointed out that an energy-dependent state-selective measurement of the RR

[*]Present address: School of Basic Sciences, Indian Institute of Technology Bhubaneswar, Bhubaneswar, 751007, India.

process would provide a more stringent test of corresponding theories, particularly in the case of very heavy ions where relativistic effects need to be taken into account [22].

At the same time, the x-ray spectroscopy experiments performed at the electron cooler of the Experimental Storage Ring (ESR) with AU^{79+} and U^{92+} ions [25–29] demonstrated the importance of observing the direct RR for precisely extracting quantum electrodynamical (QED) effects in high-Z ions. In particular, the observation of RR to the K shell, and of Lyman lines being the result of RR to high Rydberg states followed by deexcitation cascades provided the most precise measurements of the ground-state Lamb shift in H-like ions [29]. Further shell selective RR experiments detecting recombination into K and L shells were performed under cooling conditions, i.e., at zero average relative electron-ion energies. In these experiments it was shown that even in such ultimately low-energy collisions relativistic effects are important [5]. The importance of relativistic and high multipole effects for proper interpretation of radiative recombination data at high electron energies, especially for heavy and highly charged ions, has also been demonstrated during the past decades (see [30] and references therein).

In this paper we report on the first subshell-selective x-ray study of RR of bare uranium ions with electrons in an electron cooler at low nonzero relative electron-ion energies. X-ray emission from recombination into the K shell and the L subshells was recorded for seven different relative electron-ion velocities in the energy range 0–1 eV, including cooling conditions ($\langle v_{\rm rel}\rangle = 0$). Thus, the present experiment provides greatly improved access to the physics of the RR process. In particular, quite accurate quantification of the RR rate coefficient for "cooling" conditions was obtained by measuring the energy dependence of RR rate coefficients in a wider energy range. As will be demonstrated in this paper, our experimental approach with changing the relative electron-ion energy, allowed us to study the influence of relativistic effects on RR in fine detail. As a consequence, the interpretation of the experimental results was performed by comparison with nonrelativistic and fully relativistic calculations of the RR cross sections. In order to enable such an assessment in great detail, the cross sections were converted to rate coefficients using an anisotropic velocity distribution of the electrons. Likewise, the corresponding changes in the photon emission characteristics for different energies were taken into account.

II. EXPERIMENT

The experiment was performed at the electron cooler of the ESR of the GSI Helmholtzzentrum für Schwerionenforschung (GSI) in Darmstadt, Germany. Bare uranium ions extracted from the UNILAC-SIS accelerator complex were injected into the ESR at an ion energy of 360 MeV/u, phase-space cooled using electron cooling, decelerated down to 23.3 MeV/u, and electron-cooled again in order to guarantee a good beam quality during the measurements. The deceleration technique implemented at the ESR has been described previously [31]. In the present experiment the electron cooler served a twofold task: first, phase-space cooling of the ion beam and, second, the cooler was used as a target of electrons to study the RR process. The electron current and the voltage applied for cooling the

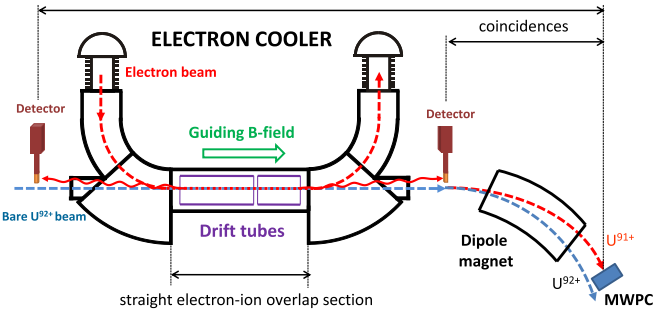

FIG. 1. (Color online) Scheme of the experimental setup at the ESR storage ring showing the electron cooler, x-ray detectors, dipole magnet, and particle detector [multiwire proportional counter (MWPC)]. True RR photons were distinguished from background events as coincidences between the x-rays and recombined U^{91+} ions registered in the MWPC.

ions at the measurement energy were 93 mA and 12.75 kV, respectively. The cooler electron beam usually is described in terms of an anisotropic Maxwell-Boltzmann distribution with transversal and parallel temperatures $T_\perp$ and $T_\parallel$, respectively [32]. Throughout, in this paper $kT_\perp = 120$ meV (in energy units) and $kT_\parallel = 0.1$ meV are used for the ESR cooler [33]. The electron-guiding magnetic field in the electron cooler was 70 mT. The total length of the straight section of the electron cooler, that is, the interaction zone, was 250 cm. The x rays arising from the RR processes in the electron-ion overlap region, were measured by two germanium detectors (see Fig. 1). The detectors were mounted in front of and behind the electron cooler at a distance of about 4.1 m from the center of the cooler interaction region. They were placed close to the ion beam at an angle of about 0.5° from the ion-beam axis. The efficiencies of the detectors for x-ray energies between 15 and 350 keV were determined using absolutely calibrated radioactive x-ray sources.

In order to suppress the strong background of photons (mainly bremsstrahlung) emitted from the electron beam, the x rays were registered in coincidence with the down-charged recombined U^{91+} ions. The recombined H-like uranium ions were separated from the coasting primary beam of bare uranium ions in the dipole magnet right after the electron cooler, and were detected by a position sensitive particle detector—in this case a gas-filled multiwire proportional counter (MWPC)—placed at a suitable position behind the dipole magnet. The measurements were performed at electron cooling conditions ($\langle v_{\rm rel}\rangle = 0$) and, additionally, at six off-cooling electron velocities. The relative energy between electrons and ions was varied by swiftly and precisely applying voltages of ±60V, ±100V, ±220 V to cylindrical drift tubes located in the overlap section of the two beams. The voltages decelerate or accelerate the electrons but leave the ion beam unaffected. The changes in the electron energy lead to collision energies in the center-of-mass frame of $E_{\rm rel} = 69.55$, 192.9, 929.2 meV (for positive voltages: $\langle v_{\rm rel}\rangle > 0$) and $E_{\rm rel} = 69.89$, 194.4, 945.6 meV (for negative voltages: $\langle v_{\rm rel}\rangle < 0$).

The off-cooling energies were chosen such that they are larger than the thermal energy associated with the transversal electron beam temperature ($E_{\rm rel} \geqslant kT_\perp$). For these energies,

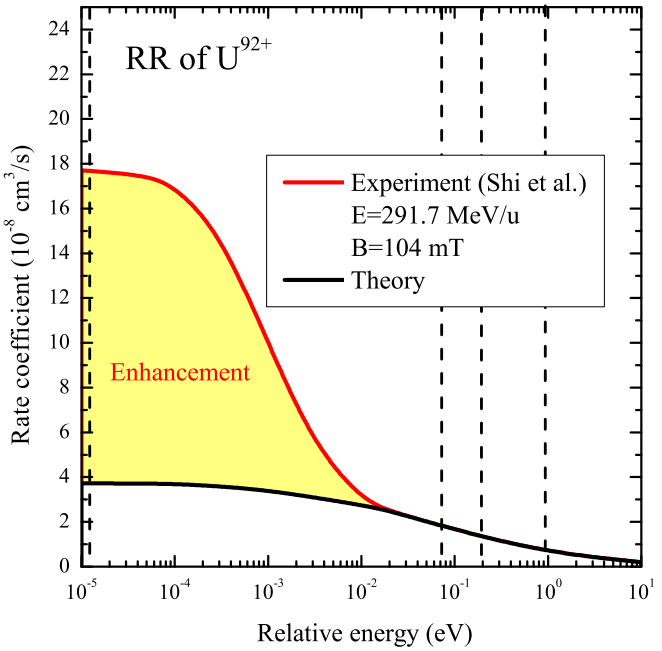

FIG. 2. (Color online) Absolute recombination rate coefficients of U^{92+} plotted versus relative energy between the electron and the ion beam compared with theoretical predictions [22]. In the experiment of Shi *et al.* the ion beam energy was 291.7 MeV/u and the magnetic guiding field strength 104 mT. The black solid line, representing theory, was calculated with $kT_{\perp} = 120$ meV and $kT_{||} = 0.1$ meV [22]. In the present experiment, *K*-RR and *L*-RR x-ray data were recorded using 23.3 MeV/u U^{92+} for cooling conditions and relative energies of 69.55, 192.9, and 929.2 meV (horizontal dashed lines). The magnetic guiding field strength was 70 mT.

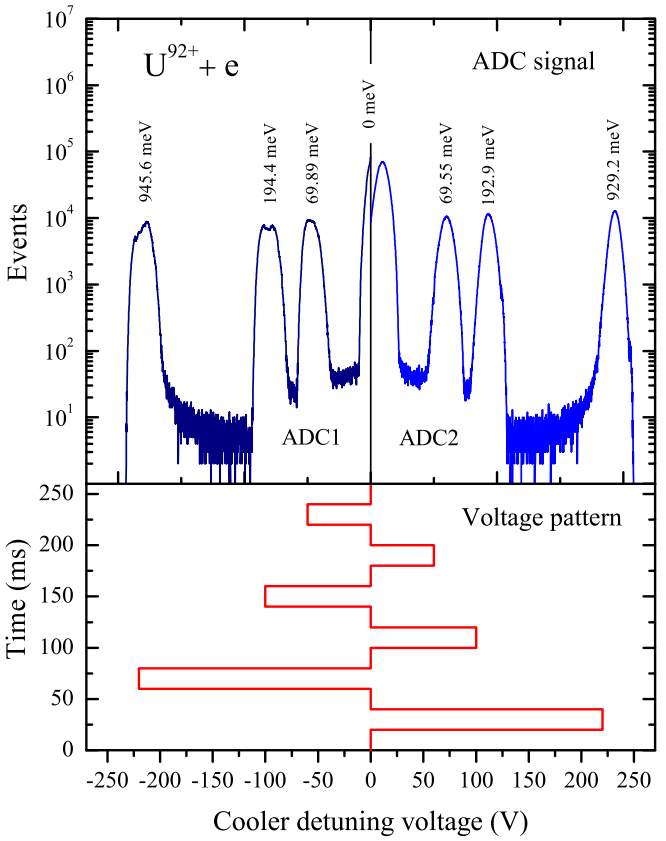

FIG. 3. (Color online) The recombination events recorded with the MWPC versus drift-tube voltages measured with an ADC and "maeander" voltage pattern (see text) applied to the drift tubes that change the electron energy (lower panel).

the aforementioned enhancement effect (cf. Sec. I and Fig. 2) was not observed in previous experiments and hence does not influence our x-ray studies. In order to avoid beam dragging effects of the electrons acting on the ions, which could change the relative energy between electrons and ions to a lower value, and to maintain good beam quality, the drift-tube voltage was changed swiftly (rise time ∼1 ms) and in a meandering voltage-time pattern. After 25 ms measurement at off-cooling energy, the electron energy was put back to its cooling value for 25 ms and then the same voltage of opposite polarity was applied for 25 ms. Experimental data were continuously collected and stored in event mode, thus allowing for a detailed off-line analysis. The corresponding pattern of applied voltages, and the measured voltages versus the RR count rate in the MWPC is displayed in Fig. 3.

A. X-ray spectra

The x rays emitted during RR of U^{92+} ions with electrons in the electron cooler were measured by two germanium detectors. The raw x-ray spectra registered for cooling and off-cooling electron velocities by the detectors placed at angles 0.5° and 179.5° are shown in Fig. 4. In the spectra one can identify the *K*-RR ($n = 1$) and *L*-RR ($n = 2$; 0.5° only) x-ray lines arising from direct radiative recombination as well as the Lyman and Balmer series populated by radiative deexcitation cascades following recombinations to higher n states. As a consequence of our coincidence approach the spectra are almost background free, because they were recorded in coincidence with the down-charged ions. Pronounced low-energy tails are observed for the Lyman x rays measured by the detector placed at the forward direction. The tails originate from the delayed emission of Lyman lines close to the front of the 0.5° x-ray detector. The delay was caused by rather slow deexcitation cascades feeding the Lyman transitions. Due to a bigger observation angle, these x-ray events had smaller Doppler-shifted photon energies. The intensity of the Lyman lines was effectively increased by the bigger detector solid angle. At the low velocity of the ions of $\beta = 0.22$ in units of speed-of-light c together with a time resolution of 20 ns the x rays emitted inside the electron cooler could be distinguished from the delayed x rays emitted close to the 0.5° x-ray detector because of their different coincidence times.

Figure 5 shows raw spectra of delayed and prompt x rays from RR. Here one finds that the spectrum of prompt x rays shows the Lyman lines without the low-energy tails, which indicates that they were emitted inside the electron cooler. On the other hand, the spectrum of delayed x rays is dominated by long-tailed Lyman and Balmer lines, while the *K*-RR and *L*-RR x rays are essentially absent. We note that the same method of x-ray spectra analysis was already successfully used in earlier experiments performed at the ESR electron cooler [5,28,29]. In contrast to previous experiments, in the present experiment

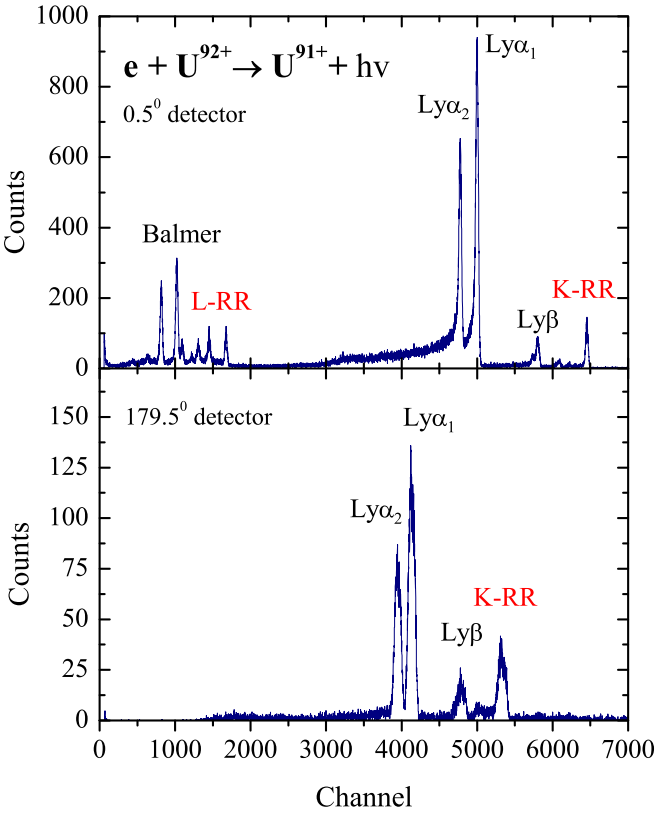

FIG. 4. (Color online) The raw x-ray spectra measured for cooling and off-cooling electron velocities by detectors placed at angles 0.5° and 179.5° showing the *K*-RR x-ray lines from direct radiative recombination to $n = 1$ shell as well as the Lyman series stemming from radiative deexcitation cascades following recombination to high Rydberg states. For the 0.5° detector also the *L*-RR lines ($n = 2$) from direct recombination and the Balmer series from cascades are visible.

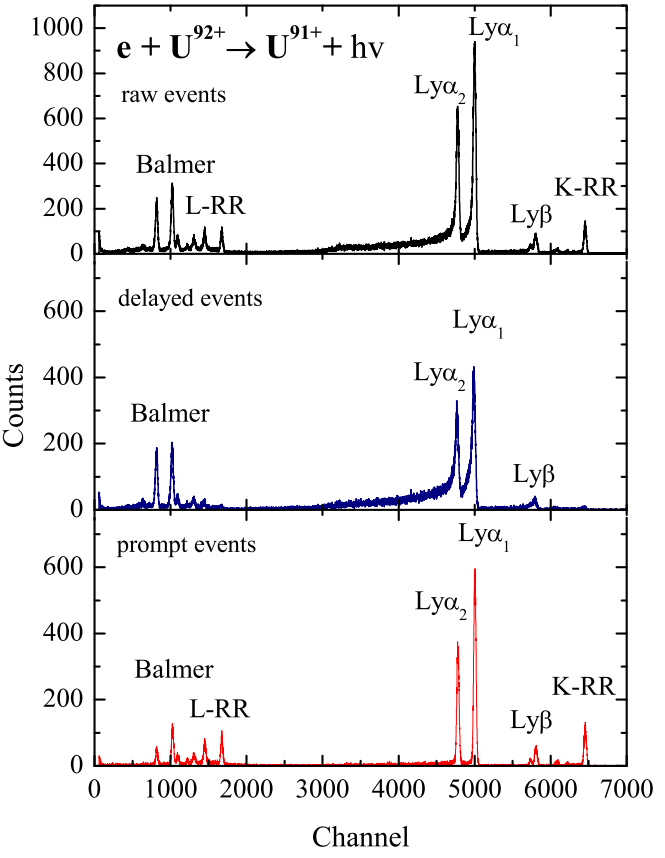

FIG. 5. (Color online) The x-ray spectra measured at 0.5° in coincidence with down-charged ions (raw spectrum). The x rays emitted just in front of the 0.5° x-ray detector (delayed events) can be distinguished from the x rays emitted in the electron cooler (prompt events), by setting an appropriate time window in the time spectrum.

the x rays were measured also by a detector placed in the backward direction at 179.5°. In this case, as one expects, the Lyman lines show no low-energy tails.

In order to obtain the RR x-ray spectra for a given relative electron energy, the prompt x-ray events coincident with registered down-charged particles were attributed to one of the analog-to-digital converter (ADC) voltage peaks (Fig. 3). As an example the x-ray spectrum measured at 0.5° and a relative energy of 69.5 meV is shown in Fig. 6. Such x-ray spectra were used to determine the RR rate coefficient for the discussed *K*-RR and *L*-RR processes.

B. Relative ion-electron energy

In the present experiment the relative electron-ion energies were varied by applying voltage to the drift tubes in the electron cooler. In this case the electron kinetic energy E_e is determined by the negative electron gun potential U_{gun} and the drift-tube voltage U_{drift} as follows:

$$E_e = -eU_{\text{gun}} + eU_{\text{drift}} + eU_{\text{space}}. \qquad (2)$$

Here U_{space} is the space charge potential resulting from the presence of the electron beam on the axis of the drift tube. Assuming uniform current density in the electron beam in an

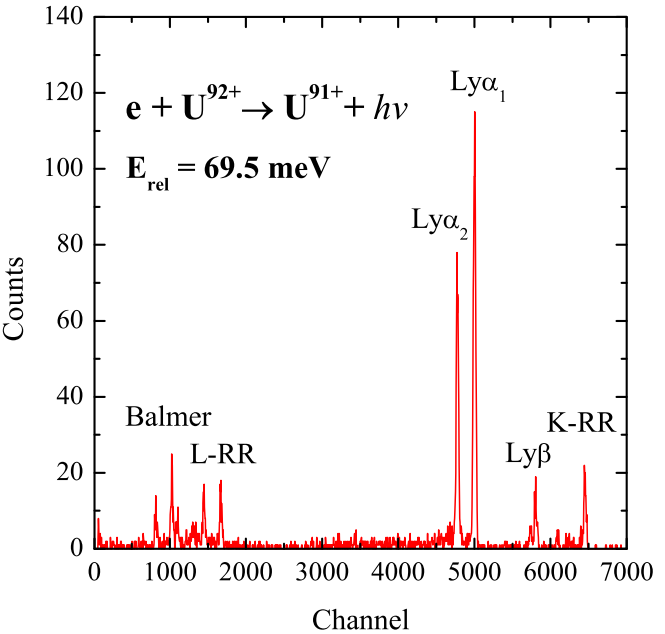

FIG. 6. (Color online) The x-ray spectrum measured at 0.5° and relative energy of 69.5 meV. Events from the delayed x-ray transitions have been excluded from this spectrum (see text).

infinitely long tube one obtains

$$U_{\text{space}} = -\frac{I_e r_e m_e c^2}{e v_e}(1 + 2ln(b/a)), \tag{3}$$

where I_e is the electron current and r_e the classical electron radius. The quantities e, m_e, and v_e are the electron charge, mass, and velocity while a and b are the radii of the electron beam and the drift tube, respectively. For the electron current used in the present experiment ($I_e = 93$ mA) the space charge potential on the axis of the drift tubes U_{space} was equal to -16 eV.

At cooling condition ($\langle v_e \rangle = \langle v_{\text{ion}} \rangle$) the energy of the ions can be calculated from the kinetic energy E_{cool} of the cooling electrons:

$$E_i = (m_i/m_e)E_{\text{cool}}, \tag{4}$$

where m_i is the ion mass. The electron energy E_e [see Eq. (2)] corrected for the drift-tube voltage and space charge potential, and the ion energy E_i determine the relative electron-ion energy:

$$E_{\text{rel}} = \mu c^2\left[\gamma_i\gamma_e - \sqrt{(\gamma_i^2 - 1)(\gamma_e^2 - 1)}\cos\theta - 1\right], \tag{5}$$

where $\mu = m_e m_i/(m_e + m_i)$ is the reduced mass of the electron-ion pair, θ is the angle between electron and the ion beams, and γ_i, γ_e are

$$\gamma_i = 1 + \frac{E_i}{m_i c^2} \qquad \gamma_e = 1 + \frac{E_e}{m_e c^2}.$$

From Eq. (5) one finds that for fixed ion energy the relative ion-electron energy depends only on two quantities, namely, the angle θ between ion and electron beam and the electron energy which is derived from the cathode voltage of the cooler and the applied drift-tube voltage. Along the electron cooler axis neither the drift-tube potential nor the interaction angle are constant for a given setting. The drift tube covers only 2 m of the total 2.5-m overlap length. The interaction angle is altered by imperfections of the homogeneity of the cooler solenoid and due to the toroidal B fields used to merge and demerge the two beams [22,33–35].

In order to account for the variation of the electric potential along the axis of drift tubes, in particular at their ends, position-dependent relative electron energies were calculated using the expected z dependence of the electric potential on the axis of a finite-length drift tube, given by [36]

$$U_{\text{drift}}(z) = \frac{V_1 + V_2}{2} - \frac{V_2 - V_1}{2}\tanh\left[\frac{1.318}{b}z\right], \tag{6}$$

where $V_1 = 0$ is the potential of the grounded beampipe, V_2 is the applied drift-tube voltage, b is the drift-tube radius, and z denotes the position in the straight electron-ion overlap section of the electron cooler with $z = 0$ in the center of the interaction region (see Fig. 7).

In addition, the interaction angle also depends on the position z inside the cooler since the electrons follow the B-field direction. Predominantly, the merging and demerging leads to interaction angles significantly different from zero. Moreover, small imperfections of the main solenoid are taken into account using B-field directions from a field mapping. The interaction angles from the B-field distribution can be found in [33] or more recently in [35]. The results were used in this paper to determine the relative electron energies. For the present experiment the position-dependent relative ion-electron energies $E_{\text{rel}}(z)$ in the electron cooler were obtained from Eq. (5) using z-dependent $\gamma_e(z)$ and $\theta(z)$.

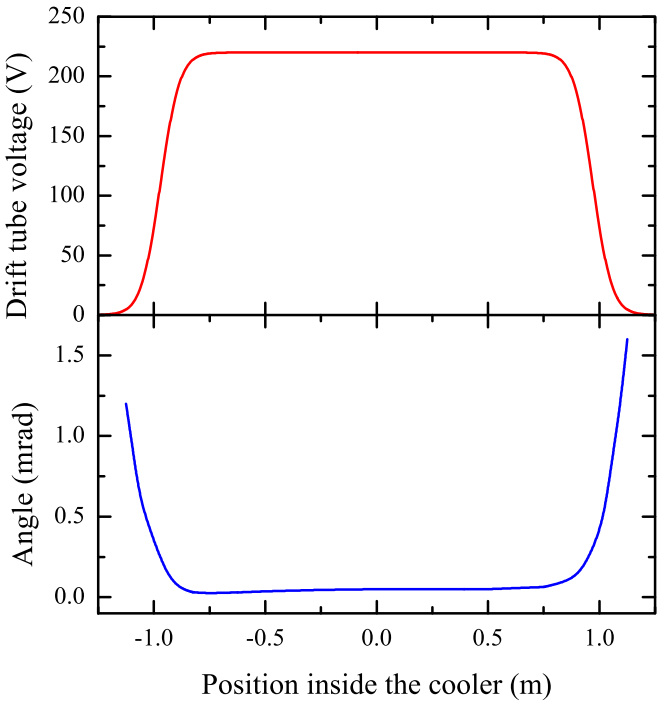

FIG. 7. (Color online) Dependence of the drift-tube potential on axis and angle θ between ion and electron (magnetic field) directions on the position inside the electron cooler (z) [22,33,34].

In Fig. 8 the resulting z dependence of the relative electron-ion energies in the electron cooler are shown for selected

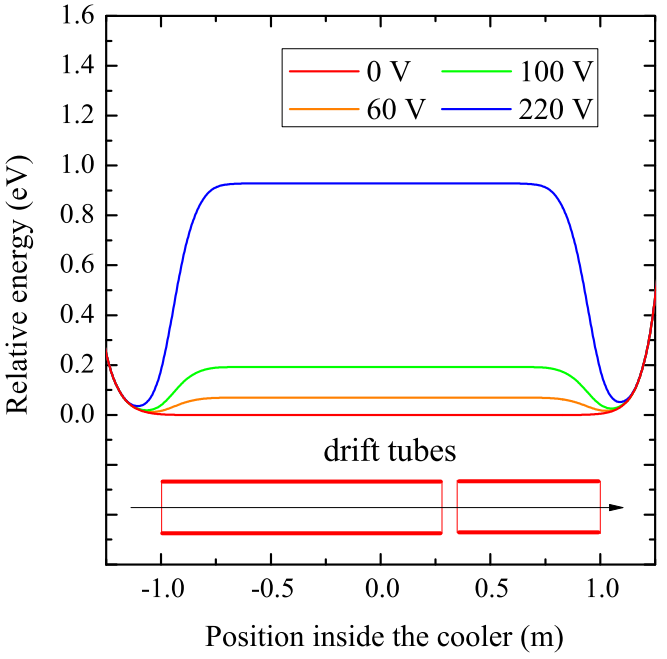

FIG. 8. (Color online) Calculated relative electron energies for different voltages applied to the drift tubes resulting from the electric potential distribution and beam misalignment along the electron cooler.

values of the drift-tube voltage. These energies were used for calculating the theoretical rate coefficients to interpret the measured RR rates (see Sec. III). As can be seen from the figure, the calculated distribution of relative energies for a given drift-tube voltage contains contributions of relative energies that are considerably lower than the set voltage, in particular, close to the drift-tube ends. The impact of the distribution of relative energies was found to be important mainly for higher nominal relative energies, that is, for higher drift-tube voltages. Since the RR cross section increases strongly with decreasing $E_{\rm rel}$ the according rate coefficient at nonzero drift-tube voltages is significantly increased due this admixture of lower energies. We note here that this effect was fully accounted for in the evaluation of the RR rate coefficient shown in the following sections.

III. RR RATE COEFFICIENTS

The RR of high-z bare ions with cooling electrons can be treated within the nonrelativistic dipole approximation. Bethe and Salpeter [2] derived a simple formula for the RR cross section to a given shell of a hydrogenlike atom with principal quantum number n. This cross section, as a function of the electron energy E in the ion frame, has the following form:

$$\sigma_{\rm RR}(E) = \sigma_0 \frac{G_n E_0^2}{nE[E_0 + n^2 E]}, \tag{7}$$

where $\sigma_0 = 2.1 \times 10^{-22}{\rm cm}^2$, $E_0 = Z^2\mathcal{R}$ is the binding energy of an electron in the K shell of an H-like atom with nuclear charge Z, and $\mathcal{R} = 13.6$ eV is the Rydberg energy. Since the classical Bethe-Salpeter formula is valid only for high n the so-called Gaunt factor G_n is introduced in Eq. (7) in order to account for deviations of this cross section from the correct quantum result for low n.

The electron energy in the ion frame appearing in Eq. (7) can be expressed in terms of its relative velocity v as follows:

$$E(v) = m_e c^2 \left[\frac{1}{\sqrt{1 - \left(\frac{v}{c}\right)^2}} - 1 \right]. \tag{8}$$

The relative electron velocity v has two components, namely, the *collective* longitudinal velocity $v_{\rm rel}$ given by the settings of the electron cooler (see Sec. II B) and the longitudinal $v_\parallel$ and transverse $v_\perp$ components of *thermal* electron velocity $\boldsymbol{v} = (v_\parallel, v_\perp)$. Thus, in Eq. (8) $v^2 = (v_{\rm rel} + v_\parallel)^2 + v_\perp^2$ where

$$v_{\rm rel} = c \sqrt{1 - \frac{1}{\left(1 + \frac{E_{\rm rel}}{m_e c^2}\right)^2}}, \tag{9}$$

with the relative ion-electron energy $E_{\rm rel}$ given by Eq. (5).

In the electron cooler the electrons have a flattened Maxwellian distribution of thermal velocities in the ion frame, $f(v_{\rm rel}, \boldsymbol{v})$, centered at the relative velocity $v_{\rm rel}$. In the experiment an RR rate coefficient $\alpha_{\rm RR}(\theta_{\rm lab}, v_{\rm rel})$, depending on the photon emission angle $\theta_{\rm lab}$ in the laboratory frame and the actual electron-ion velocity $v_{\rm rel}$ is measured. The RR rate coefficient can be derived by a convolution of the angle-differential RR cross sections $d\sigma_{\rm RR}/d\Omega$ with the thermal distribution of electron velocities [32]:

$$\alpha_{\rm RR}(\theta_{\rm lab}, v_{\rm rel}) = \left\langle v \frac{d\sigma_{\rm RR}(\boldsymbol{v})}{d\Omega} \right\rangle = \int v \frac{d\sigma_{\rm RR}(\boldsymbol{v})}{d\Omega} f(v_{\rm rel}, \boldsymbol{v}) d^3\boldsymbol{v}. \tag{10}$$

The flattened ($kT_\parallel \ll kT_\perp$) Maxwellian velocity distribution of electrons in the electron cooler is expressed, in the ion rest frame, as follows:

$$f(v_{\rm rel}, \boldsymbol{v}) = \frac{m_e}{2\pi k T_\perp} \sqrt{\frac{m_e}{2\pi k T_\parallel}} \exp\left[-\frac{m_e v_\perp^2}{2kT_\perp} \right] \times \exp\left[-\frac{m_e (v_\parallel - v_{\rm rel})^2}{2kT_\parallel} \right]. \tag{11}$$

Two theoretical approaches have been applied to evaluate the angle-differential RR cross section. First, we used the nonrelativistic dipole approximation [1,37] which is expected to be adequate for low-energy electrons. Additionally, the dipole approximation gives a simpler insight into the studied RR process. In particular, in the low-energy approximation ($E \ll E_{nl}$), i.e., when the electron energy is much smaller than electron binding energy of the final state, the angular dependence of the RR cross section is described by [37]

$$\frac{d\sigma_{\rm RR}(\boldsymbol{v})}{d\Omega} = \frac{\sigma_{\rm RR}(E_{\rm cm}(v))}{4\pi} \left[1 - \frac{\beta_{nl}}{2} P_2(\cos\vartheta) \right], \tag{12}$$

where $P_2(\cos\vartheta) = \frac{1}{2}(3\cos^2\vartheta - 1)$ is the Legendre polynomial of second order, ϑ is the angle between the electron and photon momenta (see Fig. 9), and the asymmetry parameter β_{nl} is a constant, being $\beta_{10} = 2$ for the K shell [37]. In this case the angular distribution of photons is described by the dipole term $\sin^2\vartheta$ (see Fig. 10).

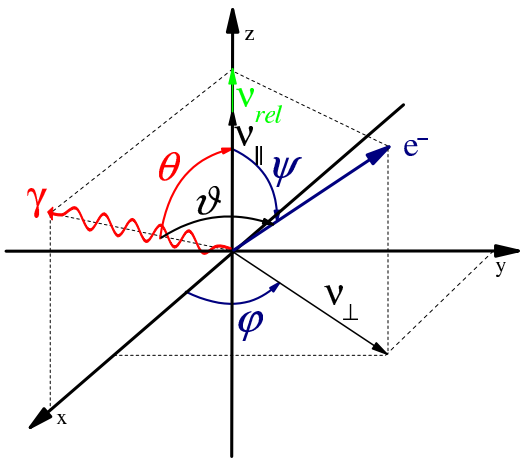

FIG. 9. (Color online) Sketch of the coordinate system considered. Ions move along the z axis, the x,z plane is the plane of the photon emission, ψ is the angle of the electron velocity vector with respect to the ion beam direction, ϑ is the angle between the electron and photon momenta, θ is the photon emission angle in the laboratory frame with respect to the ion beam direction.

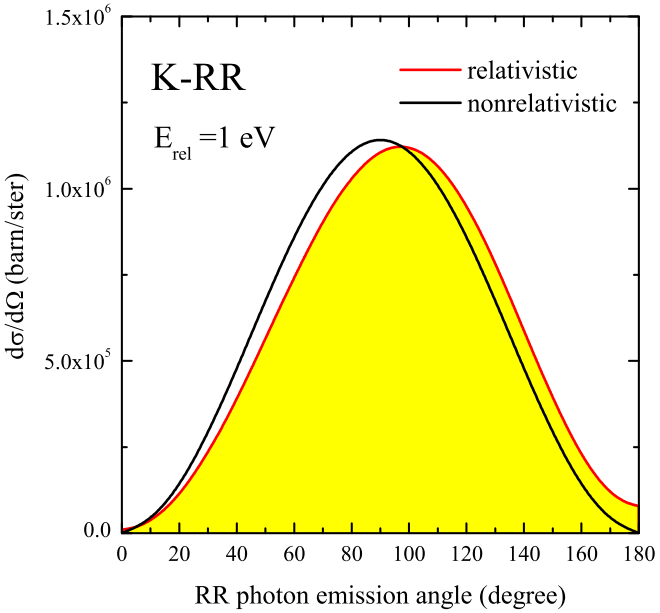

FIG. 10. (Color online) Comparison of differential RR cross sections for the K shell ($n = 1$) calculated for relative energy of 1 eV by using nonrelativistic and relativistic theory. The relativistic contributions result in the emission of recombination photons opposite the collision axis defined by the momentum of the incoming electron *as seen from the ions*. Note that for such low relative energy the maximum of the cross section distribution shifts to angles beyond 90°.

In order to express the angular distribution of RR photons with respect to the ion beam direction one finds (see Fig. 9):

$$\cos^2\vartheta = 1 - \sin^2\psi - \tfrac{1}{2}(1 - 3\sin^2\psi)\sin^2\theta, \qquad (13)$$

where ψ is the angle between the electron velocity and the ion beam direction. It can be expressed in terms of the electron velocity components:

$$\sin\psi = \frac{v_{\rm rel} + v_\parallel}{\sqrt{(v_{\rm rel} + v_\parallel)^2 + v_\perp^2}}. \qquad (14)$$

As one can see from Eq. (13), in the nonrelativistic dipole approximation the differential cross sections $\frac{d\sigma_{\rm RR}(v)}{d\Omega}$ are expressed in terms of $\sin^2\theta$ and are thus symmetric with respect to the direction perpendicular ($\theta = 90°$) to the cooler axis. At cooling conditions, that is, $\langle v_{\rm rel}\rangle = 0$ this can be easily understood taking into account that for the flattened velocity distribution of electrons in the electron cooler the electron-ion collision direction is mainly perpendicular to the electron cooler axis. The corresponding distribution of the RR photons in the ion frame is expected to have a forward-backward symmetry described by the characteristic dipole term $\sin^2\theta$.

The description of the RR process given above is valid in the moving frame of the ion and can be transformed to the laboratory system using well-known relations between photon emission angles:

$$\cos\theta = \frac{\cos\theta_{\rm lab} - \beta}{1 - \beta\cos\theta_{\rm lab}}, \qquad (15)$$

and solid angles:

$$\frac{d\Omega}{d\Omega_{\rm lab}} = \frac{1 - \beta^2}{1 - \beta\cos^2(\theta_{\rm lab})}, \qquad (16)$$

in both systems of coordinates. These transformations were used later to relate the measured and calculated RR rate coefficients.

In the present experiment the RR rate coefficients were measured by observing x-ray photons at small angles in forward and backward directions with respect to the electron cooler axis. Consequently, the intensities of the measured x rays were very sensitive to the fine details of the angular distribution of the emitted RR photons, in particular, close to angles $\theta = 0°$ and $\theta = 180°$. In this context the relativistic calculations of the RR cross sections were important, since it is well known that relativistic effects can influence the angular distribution of RR photons more strongly than the angle-integrated total cross section, even for low relative electron energies. For this reason fully relativistic calculations of the RR cross sections were performed within the framework of the Dirac theory. Within this approach the angle-differential RR cross section reads [30,38]

$$\frac{d\sigma_{\rm RR}}{d\Omega} = \frac{\hbar\omega}{8m_e c^2}\frac{\alpha\lambda_c{}^2}{\beta^2\gamma^2} \times \sum_{\mu_b m_s \lambda} |\langle\psi_{n_b\kappa_b\mu_b}|\boldsymbol{\alpha}\boldsymbol{u}_\lambda e^{-i\boldsymbol{k}\boldsymbol{r}}|\psi_{\boldsymbol{p}m_s}\rangle|^2, \qquad (17)$$

where α is the fine structure constant, m_e is the electron mass, λ_c is the Compton wavelength, and $\gamma = (1 - \beta^2)^{-1/2}$ is the Lorentz factor with $\beta = v_e/c$ denoting the reduced electron velocity. In this formula the wave functions $\psi_{n_b\kappa_b\mu_b}$ and $\psi_{\boldsymbol{p}m_s}$ are exact solutions of the relativistic Dirac equation for the bound and continuum electron, respectively. The transition operator $\boldsymbol{\alpha}\boldsymbol{u}_\lambda e^{-i\boldsymbol{k}\boldsymbol{r}}$ describes the relativistic electron-photon interaction, which accounts not only for electric dipole but also higher order (electric and magnetic) multipole terms. It is worth noting that QED corrections to the RR cross section for capture to the $n = 1$ shell of bare uranium are of the order of 1% [39]. Therefore they were neglected in the calculations. The nondipole contributions result in the emission of recombination photons opposite the collision axis defined by the momentum of the incoming electron as seen from the ion (see Fig. 10). This so-called spin-flip transition, which is forbidden within the nonrelativistic dipole approximation [1] leads, in turn, to asymmetry in the recombination rate coefficient $\alpha_{\rm RR}(\theta_{\rm lab}, v_{\rm rel})$. When the electrons are moving faster than the projectile ion ($v_{\rm rel} > 0$), the electron-ion collision axis, on average, coincides with the beam direction and, hence, K-RR photons are more likely emitted in backward directions in the laboratory frame, whereas the forward emission is predominant for $v_{\rm rel} < 0$ (that is, when the ions move faster than the electrons). As a result, in the chosen region of relative energies, the angular distribution of emitted photons strongly depends on the relative electron energy. The x-ray emission pattern changes from parallel to perpendicular to the ion beam axis (see Fig. 11).

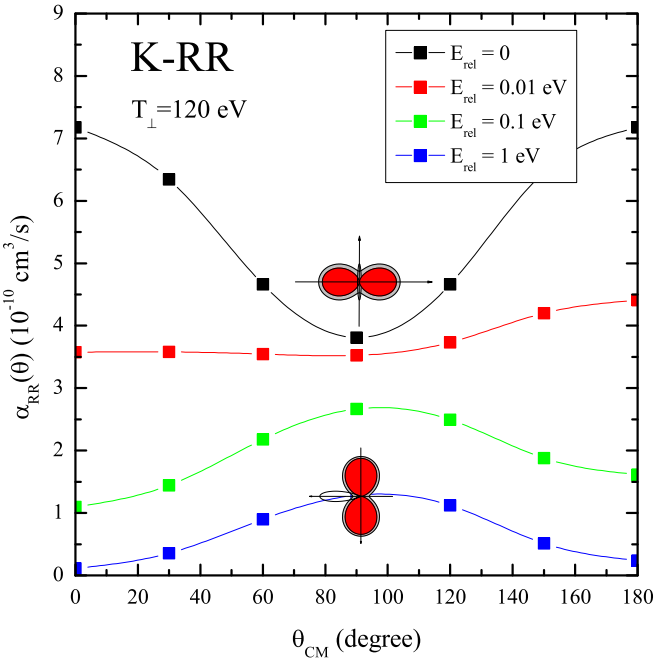

FIG. 11. (Color online) X-ray emission pattern for different relative energies obtained using fully relativistic calculations. The pattern changes from parallel for zero relative energy to perpendicular to the ion beam axis for relative energy $E_{\rm rel} = 1$ eV. $\theta_{\rm CM}$ is the photon emission angle in the center-of-mass frame.

Making use of Eq. (10), and Eq. (12) or Eq. (17) the nonrelativistic and fully relativistic angle-differential RR rate coefficients were derived from the cross sections:

$$\alpha_{\rm RR}(\theta_{\rm lab}, E_{\rm rel}) = \int_0^{2\pi}\int_0^{\infty}\int_{-\infty}^{+\infty} v_\perp\sqrt{v_\perp^2 + v_{||}^2} \times f(\boldsymbol{v}, v_{\rm rel})\frac{d\sigma_{\rm RR}(\boldsymbol{v})}{d\Omega} d\varphi dv_\perp dv_{||}. \quad (18)$$

In order to compare the experimental rate coefficient measured for a given nominal relative energy, obtained by setting the voltages in the electron cooler, the actual distribution of relative electron energies $E_{\rm rel}(z)$ in the electron cooler has to be considered (see Fig. 8 and earlier discussion). In order to account for this distribution, the theoretical predictions of the RR rate coefficients were integrated over the relative electron energy distribution, as a function of the ion position z in the electron cooler:

$$\alpha_{\rm RR}^{\rm exp}(\theta_{\rm lab}, E_{\rm rel}) = \frac{1}{L}\int_{-L/2}^{L/2} \alpha_{\rm RR}(\theta_{\rm lab}, E_{\rm rel}(z))dz. \quad (19)$$

In this way the effective values of angle-differential RR rate coefficients were calculated taking into account the variation of the electron relative energy along the interaction zone of length L in the electron cooler. The obtained values were compared with the experimental RR rate coefficients.

IV. RESULTS AND DISCUSSION

The measured rate coefficients for RR into the K and L shells in the energy range 0–1000 meV were compared with theoretical predictions based on the nonrelativistic and relativistic angle-differential RR cross sections for a flattened ($kT_{||} \ll kT_\perp$) Maxwellian velocity distribution described with temperatures $kT_\perp = 120$ meV and $kT_{||} = 0.1$ meV. The calculations of the RR rate coefficients showed that the transverse electron temperature has a significant influence on the calculated rate coefficient—it changes the value for the absolute RR rate coefficient and also the shape, in particular, for the lowest electron energies. In contrast, the longitudinal electron beam temperature $T_{||}$ has only a small influence on the calculated RR rate coefficient. We found that modifications of the longitudinal temperature in the range $\Delta kT_{||} = 0.1$ mV $\pm$ 0.05 mV change the absolute value of the RR rate coefficient but practically do not change the shape. Similarly, we checked a possible influence of the uncertainty of determining the x-ray detector angle on the RR rate coefficient and we found that changing the angle in the range $\Delta\theta_{\rm lab} = 0.5^\circ \pm 0.2^\circ$ practically does not change the calculated rate coefficients.

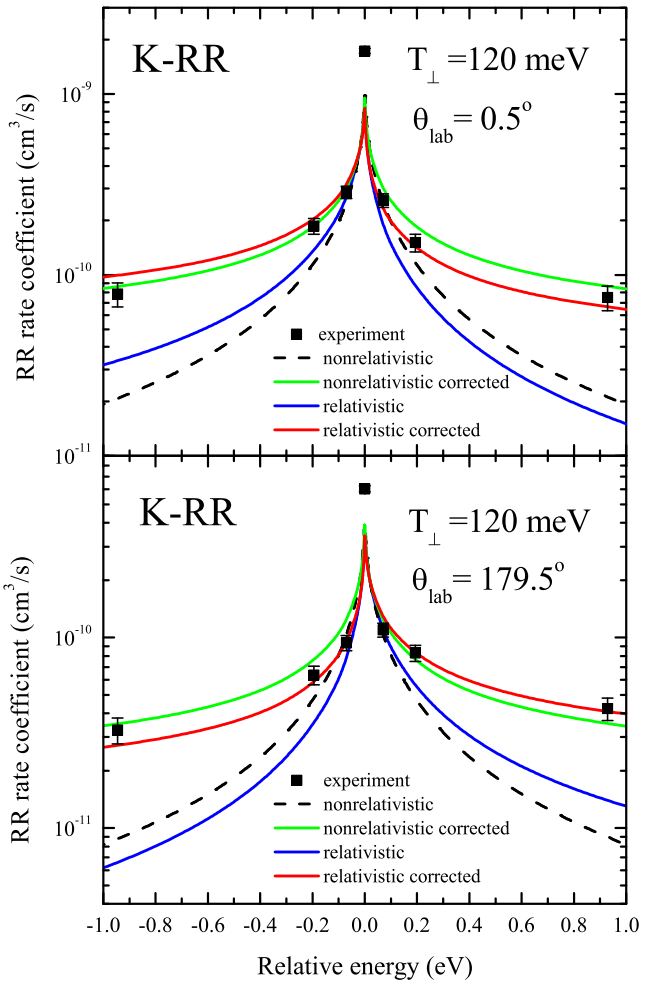

FIG. 12. (Color online) The K-shell RR rate coefficient for different relative electron energies measured by detectors placed at 0.5° and 179.5°. The data are compared with the predictions of relativistic [40] and nonrelativistic [1,37] calculations assuming the electron beam transverse temperature of $kT_\perp = 120$ meV. The description "corrected" means the calculations with Eq. (19) applied. Negative (positive) relative energy means the ions are faster (slower) then the electrons.

In order to compare the measured and the calculated RR rate coefficients in the electron energy range 0–1000 meV the experimental rate coefficients were normalized to the relativistic theory predictions, which were corrected for the distribution of the relative electron-ion energies along the electron cooler [see Eq. (19) and Fig. 8], by multiplying the data with a constant normalization factor. The measured RR rate coefficient for zero relative energy ($E_{\rm rel} = 0$) was excluded from the fitting since for the cooling condition the results could be affected by the aforementioned recombination enhancement effect.

The measured dependence of the rate coefficient for K-shell RR of U^{92+} ions with electrons in the energy range 0–1000 meV is shown in Fig. 12. The experimental K-RR rate coefficients shown in this figure are compared with the predictions of the nonrelativistic dipole approximation [1,37] and fully relativistic calculations [40]. The calculated K-RR rate coefficients, which were corrected for the variation of the relative electron energy along the electron cooler (see Fig. 8), better reproduce the energy dependence of the measured K-RR rates for off-cooling energies ($E_{\rm rel} \neq 0$) if the relativistic effects are taken into account, which is confirmed by a chi-squared test. Generally, the relativistic calculations, in contrast to the nonrelativistic ones, predict an asymmetry of the RR rate coefficients for the K shell with respect to zero relative energy, i.e., the electron cooling condition. This prediction is supported by the experimental results as shown in Fig. 12. The expected asymmetry is very small for relative energies $E_{\rm rel} < 0.1$ eV and becomes increasingly more important for increasing relative energies. The interpretation of this effect is related to the asymmetry of the relativistic RR cross section due to the spin-flip effect (see Fig. 10). Consequently, for very low relative electron energies ($E_{\rm rel} < kT_\perp$) the momenta of electrons for a flattened Maxwellian velocity distribution are predominantly *perpendicular* to the electron cooler axis and thus the observed photons are emitted along this direction, i.e., at angle $\vartheta = 90^\circ$ where the relativistic effects are rather small. On the other hand, for higher relative electron energies ($E_{\rm rel} \gg kT_\perp$) their momenta are nearly *parallel* to the electron cooler axis and the observed photons are emitted at angles close to $\vartheta = 0^\circ$ ($v_{\rm rel} > 0$) and $\vartheta = 180^\circ$ ($v_{\rm rel} < 0$), i.e., at angles where the relativistic effects cause the strongest difference. In fact, this is the reason for the observed asymmetry in the measured dependence of the K-shell RR rate coefficient upon the relative electron energy.

For the radiative recombination to the L shell the rate coefficients were measured for the $L_{1,2}$ subshells ($2s_{1/2}$,$2p_{1/2}$) and the L_3 subshell ($2p_{3/2}$). The individual contributions of the L_1 and L_2 subshells could not be resolved in the measured x-ray spectra (see Fig. 5) since the $L_{1,2}$ subshells are only separated by 75 eV which is much less than the resolution of a typical germanium detector in this energy range. The measured RR rate coefficients for the $L_{1,2}$ and L_3 subshells for the studied electron energy range $E_{\rm rel} = 0$–1000 meV are shown in Figs. 13 and 14, respectively, where they are compared with theoretical predictions of RR obtained from both nonrelativistic and fully relativistic calculations. The measured RR rate coefficients for the L shell show a weaker asymmetry with respect to the electron cooling energy ($E_{\rm rel} = 0$) than the ones for the K shell. This can

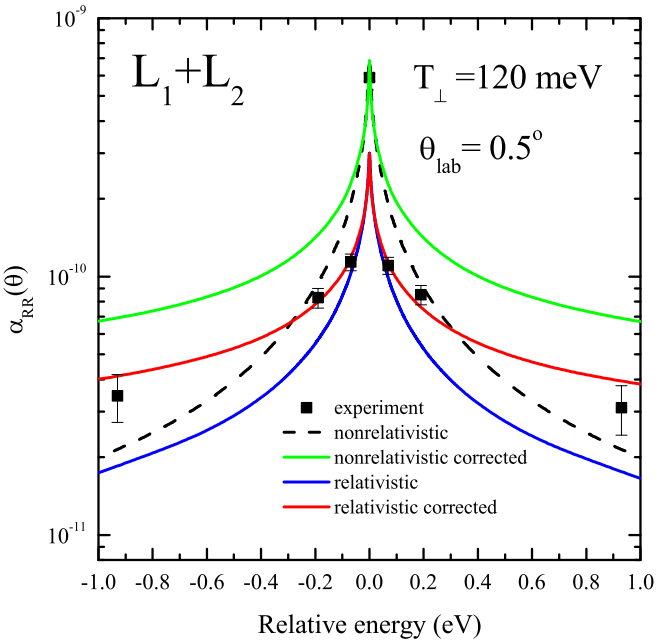

FIG. 13. (Color online) The $L_{1,2}$-subshell RR rate coefficient measured versus the relative electron energy by the x-ray detector placed at 0.5°. The data are compared with the predictions of the relativistic [40] and nonrelativistic [1,37] calculations assuming the electron beam transverse temperature $kT_\perp = 120$ meV. Negative (positive) relative energy means the ions are faster (slower) than the electrons.

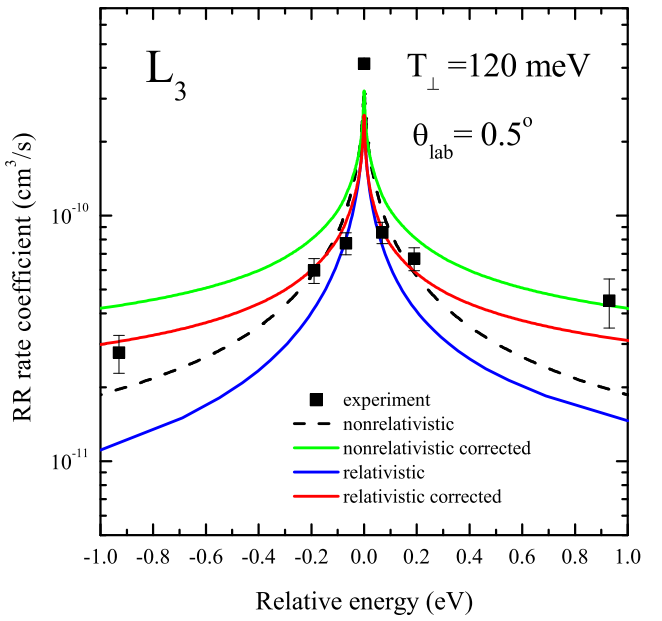

FIG. 14. (Color online) The L_3-shell RR rate coefficient measured versus the relative electron energy by the x-ray detector placed at 0.5°. The data are compared with the predictions of the relativistic [40] and nonrelativistic [1,37] calculations assuming the electron beam transverse temperature $kT_\perp = 120$ meV. Negative (positive) relative energy means the ions are faster (slower) than the electrons.

be understood as a result of nonzero RR cross sections at $\vartheta = 0^\circ$ and $\vartheta = 180^\circ$ angles for recombination to the p states [37]. Consequently, the relativistic effects do not influence the forward-backward asymmetry as much as for the s state in the K shell. This also partly explains the slightly different asymmetry observed for the $L_{1,2}$ subshells, being a mixture of s and p states, and the L_3 subshell which is a p state.

In general, the fully relativistic calculations of RR performed for the K and L shells describe the measured rate coefficients reasonably well (within $\pm 20\%$) for off-cooling electron energies ($E_{\mathrm{rel}} \neq 0$), reproducing the observed asymmetry with respect to zero relative electron energy ($E_{\mathrm{rel}} = 0$). Based on this overall good agreement for nonzero collision energies we also estimated the magnitude for RR enhancement present in our data for both the K and L shell at the zero relative electron energy. For all three cases we obtain an enhancement factor in the range of 1.5–1.8 albeit with an unknown systematic error. This systematic error stems from the very strong sensitivity of the experimental setup to the various input parameters for the correction of the theory curves with respect to the distribution of relative velocities. This correction is most sensitive for cross-section features with steep slope, in case of the RR close to 0. If this finding of an enhancement for RR into low-n shells can be verified in a dedicated experiment with a further improvement of experimental conditions, the result would be very important for a better understanding of the RR process in the electron cooler plasma.

V. CONCLUSIONS

The radiative recombination of U^{92+} ions with electrons was studied in a subshell-selective manner by observing the emitted x-ray photons from recombination into the K and L shells for relative electron energies in the range 0–1000 meV, that is, for the first time in an electron cooler at nonzero collision energies. The measured electron energy dependence of the RR rate coefficients was found to be sensitive to relativistic effects. The present experiment yielded also hints for an enhancement of RR rate coefficients into the K and L shells, i.e., into low-n shells. This new experiential method is very promising for further experimental studies, for example, with more energy steps, in particular also across and below the onset threshold of the RR enhancement.

ACKNOWLEDGMENTS

This work has been supported by I3 EURONS under EC Contract No. 506065, the Polish Ministry of Science and Higher Education under Grant No. N20215931/3048, and the Swiss National Science Foundation. A.S. acknowledges support from GSI and Helmholtz Association under Grant No. VH-NG-421. S.T. acknowledges support from German Research Foundation (DFG) under Contract No. TA 740 1-1. A.M. and C.B. acknowledge financial support from the German Federal Ministry for Education and Research (BMBF) (Contracts No. 06GI947 and No. 06GI7127/05P12R6FAN). We would like to express our thanks to the ESR team for the very good collaboration.

[1] M. Stobbe, Ann. Phys. **399**, 661 (1930).
[2] H. Bethe and E. Salpeter, *Quantum Mechanics of One- and Two-Electron Systems* (Springer, Berlin, 1957).
[3] M. Hörndl, S. Yoshida, A. Wolf, G. Gwinner, and J. Burgdörfer, Phys. Rev. Lett. **95**, 243201 (2005).
[4] M. Hörndl, S. Yoshida, A. Wolf, G. Gwinner, M. Seliger, and J. Burgdörfer, Phys. Rev. A **74**, 052712 (2006).
[5] R. Reuschl, A. Gumberidze, C. Kozhuharov, U. Spillmann, S. Tashenov, T. Stöhlker, and J. Eichler, Phys. Rev. A **77**, 032701 (2008).
[6] S. Tashenov, T. Bäck, R. Barday, B. Cederwall, J. Enders, A. Khaplanov, Y. Poltoratska, K.-U. Schässburger, and A. Surzhykov, Phys. Rev. Lett. **107**, 173201 (2011).
[7] P. Bryans, N. R. Badnell, T. W. Gorczyca, J. M. Laming, W. Mitthumsiri, and D. W. Savin, Astrophys. J. Suppl. **167**, 343 (2006).
[8] N. R. Badnell, Astrophys. J. Suppl. **167**, 334 (2006).
[9] M. B. Trzhaskovskaya, V. K. Nikulin, and R. E. H. Clark, Phys. Rev. E **78**, 035401 (2008).
[10] M. Ozawa, K. Koyama, H. Yamaguchi, K. Masai, and T. Tamagawa, Astrophys. J. **706**, L71 (2009).
[11] S. N. Nahar, Astrophys. J. Suppl. **167**, 315 (2006).
[12] Y. L. Xue, X. Cai, D. Yu, J. Shao, F. F. Ruan, D. J. Qi, M. W. Zhang, and W. Wang, J. Phys.: Conf. Ser. **163**, 012075 (2009).
[13] M. B. Trzhaskovskaya, V. K. Nikulin, and R. E. H. Clark, At. Data Nucl. Data Tables **96**, 1 (2010).
[14] S. Tashenov, D. Banaś, H. Beyer, C. Brandau, S. Fritzsche, A. Gumberidze, S. Hagmann, P.-M. Hillenbrand, H. Jörg, I. Kojouharov, C. Kozhuharov, M. Lestinsky, Y. A. Litvinov, A. V. Maiorova, H. Schaffner, V. M. Shabaev, U. Spillmann, T. Stöhlker, A. Surzhykov, and S. Trotsenko, Phys. Rev. Lett. **113**, 113001 (2014).
[15] L. H. Andersen, J. Bolko, and P. Kvistgaard, Phys. Rev. Lett. **64**, 729 (1990).
[16] A. Wolf, J. Berger, M. Bock, D. Habs, B. Hochadel, G. Kilgus, G. Neureither, U. Schramm, D. Schwalm, E. Szmola, A. Müller, M. Wagner, and R. Schuch, Z. Phys. D **21**, S69 (1991).
[17] H. Gao, D. R. DeWitt, R. Schuch, W. Zong, S. Asp, and M. Pajek, Phys. Rev. Lett. **75**, 4381 (1995).
[18] H. Gao, R. Schuch, W. Zong, E. Justiniano, D. R. DeWitt, H. Lebius, and W. Spies, J. Phys. B **30**, L499 (1997).
[19] A. Hoffknecht, T. Bartsch, S. Schippers, A. Müller, N. Eklöw, P. Glans, M. Beutelspacher, M. Grieser, G. Gwinner, A. A. Saghiri, and A. Wolf, Phys. Scr. **T80B**, 298 (1999).
[20] A. Hoffknecht, O. Uwira, S. Schennach, A. Frank, J. Haselbauer, W. Spies, N. Angert, P. H. Mokler, R. Becker, M. Kleinod, S. Schippers, and A. Müller, Phys. Scr. **T80B**, 316 (1999).
[21] G. Gwinner, A. Hoffknecht, T. Bartsch, M. Beutelspacher, N. Eklöw, P. Glans, M. Grieser, S. Krohn, E. Lindroth, A. Müller, A. A. Saghiri, S. Schippers, U. Schramm, D. Schwalm, M. Tokman, G. Wissler, and A. Wolf, Phys. Rev. Lett. **84**, 4822 (2000).

[22] W. Shi, C. B. S. Böhm, C. Brandau, A. Hoffknecht, S. Kieslich, S. Schippers, A. Müller, C. Kozhuharov, F. Bosch, B. Franzke, P. H. Mokler, M. Steck, T. Stöhlker, and Z. Stachura, Eur. Phys. J. D **15**, 145 (2001).

[23] A. Müller, S. Schennach, M. Wagner, J. Haselbauer, O. Uwira, W. Spies, E. Jennewein, R. Becker, M. Kleinod, U. Pröbstel, N. Angert, J. Klabunde, P. H. Mokler, P. Spädtke, and B. Wolf, Phys. Scr. **T37**, 62 (1991).

[24] C. Heerlein, G. Zwicknagel, and C. Toepffer, Phys. Rev. Lett. **89**, 083202 (2002).

[25] H. F. Beyer, D. Liesen, F. Bosch, K. D. Finlayson, M. Jung, O. Klepper, R. Moshammer, K. Beckert, H. Eickhoff, B. Franzke, F. Nolden, P. Spädtke, M. Steck, G. Menzel, and R. D. Desllates, Phys. Lett. A **184**, 435 (1994).

[26] D. Liesen, H. F. Beyer, K. D. Finlayson, F. Bosch, M. Jung, O. Klepper, R. Moshammer, K. Beckert, H. Eickhoff, B. Franzke, F. Nolden, P. Spädtke, M. Steck, G. Menzel, and R. D. Deslattes, Z. Phys. D **30**, 307 (1994).

[27] H. F. Beyer, G. Menzel, D. Liesen, A. Gallus, F. Bosch, R. Deslattes, P. Indelicato, T. Stöhlker, O. Klepper, R. Moshammer, F. Nolden, H. Eickhoff, B. Franzke, and M. Steck, Z. Phys. D **35**, 169 (1995).

[28] A. Gumberidze, T. Stöhlker, D. Banaś, K. Beckert, P. Beller, H. F. Beyer, F. Bosch, X. Cai, S. Hagmann, C. Kozhuharov, D. Liesen, F. Nolden, X. Ma, P. H. Mokler, A. Orsic-Muthig, M. Steck, D. Sierpowski, S. Tashenov, A. Warczak, and Y. Zou, Phys. Rev. Lett. **92**, 203004 (2004).

[29] A. Gumberidze, T. Stöhlker, D. Banaś, K. Beckert, P. Beller, H. F. Beyer, F. Bosch, S. Hagmann, C. Kozhuharov, D. Liesen, F. Nolden, X. Ma, P. H. Mokler, M. Steck, D. Sierpowski, and S. Tashenov, Phys. Rev. Lett. **94**, 223001 (2005).

[30] J. Eichler and T. Stöhlker, Phys. Rep. **439**, 1 (2007).

[31] T. Stöhlker, H. Reich, K. Beckert, F. Bosch, A. Gallus, H. Eickhoff, B. Franzke, T. Kandler, O. Klepper, C. Kozhuharov, G. Menzel, P. Mokler, F. Nolden, H. Prinz, P. Spädtke, M. Steck, T. Winkler, R. Dunford, P. Rymuza, T. Ludziejewski, Z. Stachura, P. Swiat, and A. Warczak, Hyperfine Interact. **108**, 29 (1997).

[32] H. Poth, Phys. Rep. **196**, 135 (1990).

[33] A. Hoffknecht, C. Brandau, T. Bartsch, C. Böhme, H. Knopp, S. Schippers, A. Müller, C. Kozhuharov, K. Beckert, F. Bosch, B. Franzke, A. Krämer, P. H. Mokler, F. Nolden, M. Steck, T. Stöhlker, and Z. Stachura, Phys. Rev. A **63**, 012702 (2000).

[34] W. Shi, T. Bartsch, C. Böhme, C. Brandau, A. Hoffknecht, H. Knopp, S. Schippers, A. Müller, C. Kozhuharov, K. Beckert, F. Bosch, B. Franzke, P. H. Mokler, F. Nolden, M. Steck, T. Stöhlker, and Z. Stachura, Phys. Rev. A **66**, 022718 (2002).

[35] D. Bernhardt, C. Brandau, Z. Harman, C. Kozhuharov, S. Böhm, F. Bosch, S. Fritzsche, J. Jacobi, S. Kieslich, H. Knopp, F. Nolden, W. Shi, Z. Stachura, M. Steck, T. Stöhlker, S. Schippers, and A. Müller, Phys. Rev. A **91**, 012710 (2015).

[36] M. Szilagyi, *Electron and Ion Optics* (Plenum Press, New York, 1988).

[37] M. Pajek and R. Schuch, Phys. Rev. A **45**, 7894 (1992).

[38] R. H. Pratt, A. Ron, and H. K. Tseng, Rev. Mod. Phys. **45**, 273 (1973).

[39] V. M. Shabaev, V. A. Yerokhin, T. Beier, and J. Eichler, Phys. Rev. A **61**, 052112 (2000).

[40] A. Surzhykov, P. Koval, and S. Fritzsche, Comput. Phys. Commun. **165**, 139 (2005).